Single-chip mechatronic microsystem for surface imaging and force response studies

Sadik Hafizovic, Diego Barrettino*, Tormod Volden, Jan Sedivy, Kay-Uwe Kirstein, Oliver Brand†, and Andreas Hierlemann‡

Physical Electronics Laboratory, Swiss Federal Institute of Technology (Eidgenössische Technische Hochschule), Hoenggerberg HPT-H4.2, Wolfgang-Pauli-Strasse 16, 8093 Zurich, Switzerland

Edited by Calvin F. Quate, Stanford University, Stanford, CA, and approved October 25, 2004 (received for review August 5, 2004)

We report on a stand-alone single-chip (7 × 10 mm) atomic force microscopy unit including a fully integrated array of cantilevers, each of which has an individual actuation, detection, and control unit so that standard atomic force microscopy operations can be performed by means of the chip only without any external controller. The system offers drastically reduced overall size and costs as well as increased scanning speed and can be fabricated with standard complementary metal oxide semiconductor technology with some subsequent micromachining steps to form the cantilevers. Full integration of microelectronic and micromechanical components on the same chip allows for the controlling and monitoring of all system functions. The on-chip circuitry, which includes analog signal amplification and filtering stages with offset compensation, analog-to-digital converters, a powerful digital signal processor, and an on-chip digital interface for data transmission, notably improves the overall system performance. The microsystem characterization evidenced a vertical resolution of <1 nm and a force resolution of <1 nN as shown in the measurement results. The monolithic system represents a paradigm of a mechatronic microsystem that allows for precise and fully controlled mechanical manipulation in the nanoworld.

atomic force microscopy | cantilever | complementary metal oxide semiconductor

New measurement, metrology, and imaging techniques have been pivotal to the rapid development of many branches of science such as materials science, microelectronics, and microbiology, to name a few. The invention of the scanning-tunneling microscope by Binning and Rohrer in 1982 (1) and, in particular, the invention of the atomic force microscope (AFM) in 1986 (2) have established a basis for many findings in various scientific areas over the last years. The AFM has evolved at an exceptional speed from a laboratory prototype to a commercial instrument (consider, e.g., Veeco Instruments, Woodbury, NY) and many other scanning probe techniques (3) have been developed, which will not be further mentioned here. The AFM has been used to measure forces during stretching of DNA strands (4) and rupture forces of single covalent bonds (5) and can be operated in liquids, which enables its use in biological applications (6–8). The AFM also can be used to perform surface manipulations such as lithographic fabrication of a transistor (9, 10) or AFM-based data storage (11, 12).

Commercially available AFM instruments are rather bulky and have a low throughput because of the serial nature of the involved scanning process and the limited scanning range, which renders the investigation of larger samples rather laborious. The detection of the cantilever deflection is done mostly by means of a laser, which is costly and makes the adjustment and cantilever exchange very time consuming, in particular, when operating in a vacuum environment. To overcome these limitations, AFM probes with integrated detection schemes such as capacitive (13), piezoelectric or piezoresistive schemes (10, 14–17), and high-speed scanning systems that rely on arrays of cantilevers featuring piezoelectric excitation and piezoresistive/piezoelectric readout (10, 18–20) have been developed. All of those systems, however, require a larger set of desktop equipment because no integrated electronics or functions are provided.

Materials and Methods

We report here on a stand-alone single-chip AFM unit including a fully integrated array of cantilevers, each of which has an individual actuation, detection, control, amplification, and on-chip digital processing unit as well as an individual offset compensation so that, e.g., constant-force operation is performed without any external controller. The cantilevers can be moved and precisely controlled within a range of 0.5 to 6 μm (at 0.5- to 6-nm resolution) so that the chip has only to be brought within a distance of maximally 6 μm to a surface and then can be used to carry out, e.g., multiple force-distance measurements by using the integrated electronics via a LABVIEW (National Instruments, Austin, TX) interface. Only an x-y scanning stage is necessary for imaging or lateral scanning by using one or several of the individually controlled cantilevers. The individual cantilever control is of paramount importance in using multi-cantilever arrays because there is always a slight tilt between the chip plane determining the cantilever positions and the sample surface plane so that some cantilevers are closer to the surface than others. Parallel scanning of multiple cantilevers only provides good results by implementing a fast and simultaneous individual force feedback for each scanning cantilever in a closed loop (no multiplexing).

Earlier work on integrated AFM instruments included a chip featuring up to 10 cantilevers and analog time-multiplexed actuation and readout of the cantilevers featuring rather limited force and vertical resolution (21).

The fully integrated AFM microsystem is fabricated in standard integrated-circuit technology (complementary metal oxide semiconductor, CMOS). The cantilevers of this microsystem are deflected by making use of the bimorph effect, i.e., the different thermal expansion coefficients of silicon and the aluminum layers (metal 1 and metal 2 of the CMOS process; see refs. 21 and 22). Upon heating of the layer sandwich, the cantilever bends, and the bending can be precisely controlled through the heating current passing the diffused heating resistor at the surface of the silicon. To detect the cantilever deflection upon force exerted on the tip, four piezoresistors (resistors that change their resistance upon mechanical stress) are arranged at the cantilever base in a Wheatstone-bridge configuration (15, 16, 21). Two of them are

ENGINEERING

This paper was submitted directly (Track II) to the PNAS office.

Abbreviations: AFM, atomic force microscope (microscopy); CMOS, complementary metal oxide semiconductor; DAC, digital-to-analog converter; ADC, analog-to-digital converter; DSP, digital signal processor; SAM, self-assembled monolayer.

*Present address: Microscale Life Sciences Center, Department of Electrical Engineering, University of Washington, Campus Box 352500, Seattle, WA 98195-2500.

†Present address: School of Electrical and Computer Engineering, Georgia Institute of Technology, Atlanta, GA 30332-0250.

‡To whom correspondence should be addressed. E-mail: hierlema@iqe.phys.ethz.ch.

© 2004 by The National Academy of Sciences of the USA

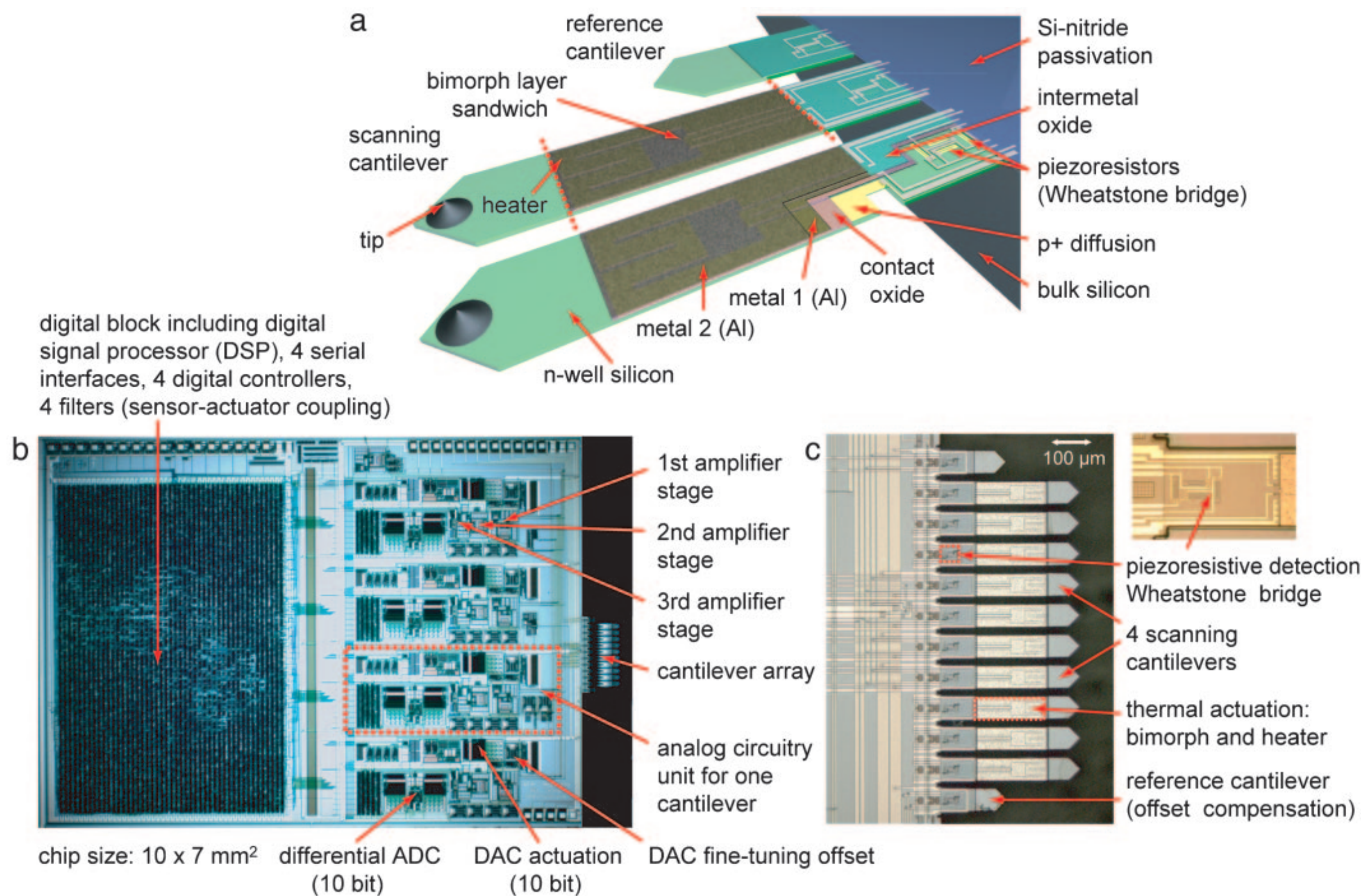

Fig. 1. Schematic and micrographs of the monolithic AFM. (*a*) 3D schematic of three cantilevers (two scanning cantilevers and one shorter reference cantilever) showing the different CMOS layers as they are used for the various cantilever components (actuation, bimorph and heater; detection, piezoresistive Wheatstone bridge). (*b*) Micrograph of the overall microsystem chip featuring the digital block on the left and four identical analog units to control the four central cantilevers on the right. The different circuitry subunits are indicated. (*c*) Close-up of the cantilever area. The chip features 12 cantilevers, 10 of which can be potentially used for scanning (500 μm long, 85 μm wide). Only the four cantilevers in the center are connected to the circuitry. The two shorter ones at the flanks (250 μm long) serve as references.

collaterally oriented to the cantilever axis, and two of them are oriented perpendicularly to achieve a maximum signal upon deflection (see Fig. 1*c Inset*) (21). A detailed 3D schematic of the scanning microcantilever is shown in Fig. 1*a*. The cantilever is 500 μm long, 85 μm wide, and 5 μm thick and features a force constant of 1 N/m. The on-chip circuitry is designed to perform the microcantilever deflection control in a vertical direction, an offset compensation, and the amplification and conditioning of the signals from the piezoresistive Wheatstone bridge. The details of this on-chip circuitry are described later. The vertical drift of the individually controlled cantilever was measured to be on the order of 10 nm/h under ambient conditions.

Functional elements of the cantilevers such as the heaters or the metal components are fabricated during the CMOS processing (0.8-μm double-metal, double-poly CMOS process of austriamicrosystems, Unterpremstaetten, Austria). The cantilever structures are then formed in subsequent micromachining steps. First, anisotropic silicon wet-etching using a potassium-hydroxide solution applied to the backside of the wafer is used to create silicon membranes. An electrochemical etch stop technique provides a defined and uniform thickness of the membrane, which consists of the n-well layer of the CMOS process (23). Front-side reactive ion etching (RIE) or wet etching is used afterward to locally remove oxide layers from the cantilever tip, then front-side RIE is used again to release the cantilevers. Finally, a silicon nitride tip (radius 10–20 nm) is mounted at the cantilever end.

Fig. 1*b* shows a micrograph of the overall microsystem chip, which features a die size of 10.00 × 7.00 mm, and Fig. 1*c* shows a close-up of the 12-cantilever array. The spacing between the cantilevers is 25 μm. The 10 scanning cantilevers, four of which are connected to the circuitry and can be individually controlled (Fig. 1*c*), are located in the center of the array. The two reference cantilevers located at the left and right ends of the array are 250 μm long, 85 μm wide, and 5 μm thick. They feature only the Wheatstone bridge for deflection detection, and they are shorter than the scanning cantilevers so they do not contact the sample surface. The reference cantilevers are used for offset compensation of the Wheatstone bridge.

The electronics covering most of the chip area include four repeated mainly analog circuitry units (Figs. 1*b* and 2), which are connected to the four central cantilevers and a common digital block, which is used for digital signal processing and includes a serial digital bus interface to connect to off-chip components. Owing to chip area constraints, only four readout and digital processing channels have been realized on-chip to provide a proof of concept. The integration of 10 readout channels can be realized by a redesign in CMOS technology with smaller feature size.

A simplified block diagram of the major circuitry units is shown in Fig. 2. The microsystem has an analog/digital mixed-

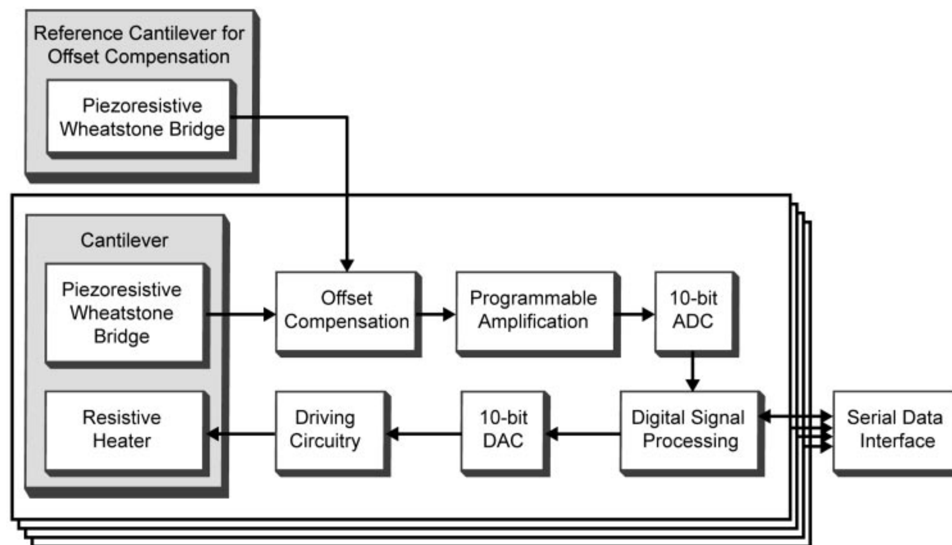

Fig. 2. Schematic of the chip architecture and the electronic components. The four frames indicate that these subunits are repeated for each active cantilever, i.e., four times. The chip also includes a DSP and a serial digital interface.

signal architecture. The cantilever deflection signal coming from the Wheatstone bridge is amplified, filtered, conditioned, and translated into the digital domain. All control operations are handled in the digital signal processor (DSP), which then issues actuation signals to the cantilever heater via a digital-to-analog converter (DAC). This way a closed-loop operation and self-controlled system is realized for every cantilever.

The circuitry unit repeated with each cantilever includes a fully differential analog amplification (three-stage amplification: fully differential low-noise programmable amplifier, programmable amplifier, and fixed-gain amplifier) and filtering unit, which provides low-noise readout and signal processing of the Wheatstone bridge signal. Multiple stages of offset compensation ensure the maximum possible force resolution to be

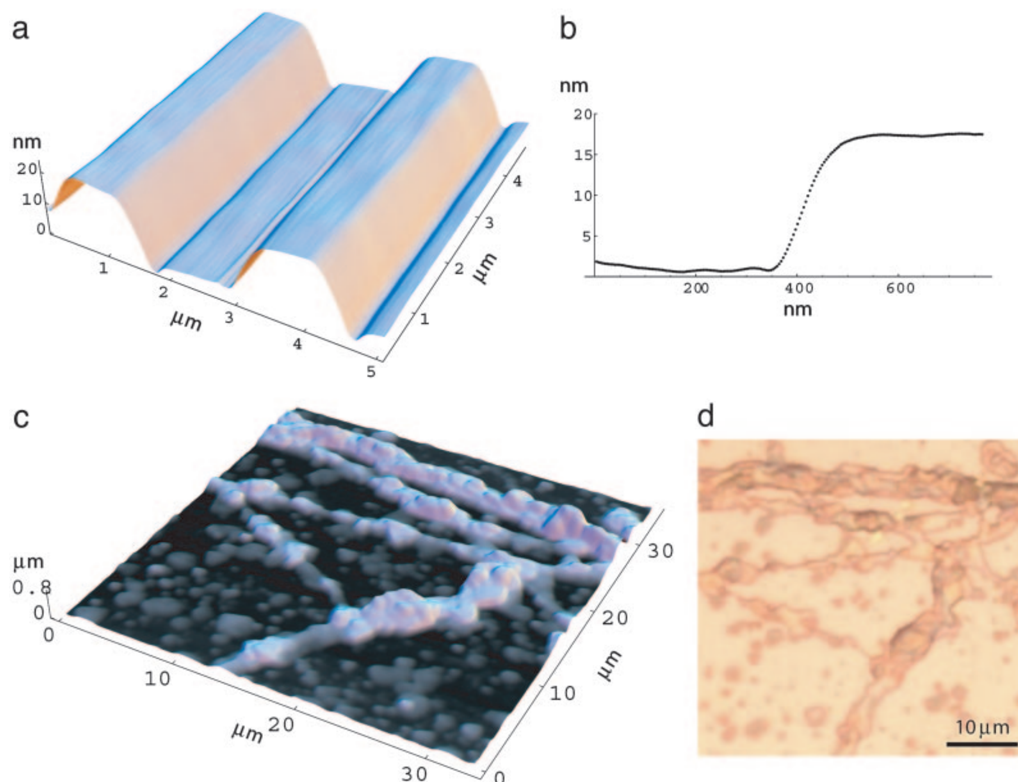

Fig. 3. Surface imaging results of the single-chip AFM. (*a*) Scanning image (constant-force mode) of a silicon grating featuring step heights of 18 nm at a 3-μm distance. A Gaussian smoothing with a radius of three data points was applied to yield the image. (*b*) High-resolution line scan over one 18-nm step. Each displayed data point represents the average of 300 values. The vertical resolution is $<$1 nm. (*c*) Scan of a biological sample at a force of 10 nN and a scanning speed of 100 μm/s representing a network of dried chicken neurites on a silicon oxide surface after fixation. (*d*) Light microscope image of the same area of a network of dried chicken neurites for comparison.

PNAS PNAS PNAS PNAS

achieved: After the first amplifier stage the coarse offset of the piezoresistive Wheatstone bridge is compensated by subtracting the offset signal of the reference cantilever structure (Fig. 1*c*). This offset is caused mainly by fabrication spread in the cantilever and the Wheatstone bridge (24) and also includes the offsets of the signal amplifiers. The imperfect matching of the diffused piezoresistive sensors from cantilever to cantilever can be compensated by another compensation stage, which enables an individual adjustment of the dc value of each readout channel with an eight-bit resolution by means of a programmable DAC. The overall gain of the analog signal processing is programmable from 18 to 44 dB to cover the whole range of expectable forces in various applications. The amplified force signal is converted by a 10-bit successive-approximation analog-to-digital converter (ADC) and fed into the DSP. The DSP unit comprises two programmable infinite-impulse-response filters, each with six coefficients, which can be configured to act as proportional-integral-derivative controllers for the constant-force imaging mode. The controllers also provide averaging functions to further improve the force resolution, and they compensate for thermal sensor-actuator crosstalk. The computing power of the DSP unit for the four cantilevers amounts to 16 million arithmetic operations per s, which is one of the highest values ever realized in CMOS-based micromechanical systems. This large value enables us to issue 100,000 actuation signals per s per cantilever for repositioning and allows for precise cantilever position control even when fast force changes are to be expected. The cantilever actuation signals coming from the DSP unit are converted to the analog domain by 10-bit flash DACs and provide, together with analog square-root circuits, linear actuation characteristics. For a total deflection range of 1 μm, a resolution of 1 nm has been achieved, which can be further improved to 0.5 nm by lowering the overall deflection range to 0.5 μm.

Results and Discussion

Two prototype applications were selected to show the performance of the monolithic AFM microsystem: (*i*) surface imaging and (*ii*) force-distance measurements.

For surface imaging, the x-y scanning function of a Nanoscope III (Digital Instruments, Santa Barbara, CA) was used, and the microsystem was operated in constant-force mode. The on-chip force controller measures the force acting on the cantilever and keeps it constant while the tip is scanned over the surface. Height information of the scanned sample is obtained from the actuation signal that is required to keep the cantilever force constant. Fig. 3*a* shows a scanning image of a silicon grating with 18-nm steps at a 3-μm distance recorded at a scanning speed of 20 μm/s and a force of 50 nN. Fig. 3*b* shows a small-range line scan recorded at 3 μm/s. The maximum possible scanning speed of the monolithic system is $\approx$1 mm/s. The maximum readout rate of the force signal is 100 kHz, which allows for averaging multiple values per data point in the DSP for better noise suppression. Each displayed data point in Fig. 3 *a* and *b* represents the average of 300 values. The measured error signal indicates an excellent tracking of the surface topography. A vertical resolution of $<$1 nm has been achieved (Fig. 3*b*). A larger area scan of a biological sample at a force of 10 nN and a scanning speed of 100 μm/s is shown in Fig. 3*c*, representing a network of dried-out chicken neurites on a silicon oxide surface after fixation. A light microscope image is given for comparison (Fig. 3*d*). The force exerted on a sample can be kept as low as 5 nN so that also soft samples can be imaged. Tapping-mode operation can be also realized with the monolithic AFM system but has not been tested so far.

In the force-distance mode, the microsystem was operated with the on-chip controllers performing the approach to and retraction from the sample surface, during which the force on the cantilever was recorded. Two force-distance measurements were conducted per s. The experimentally determined force resolution was $<$1 nN.

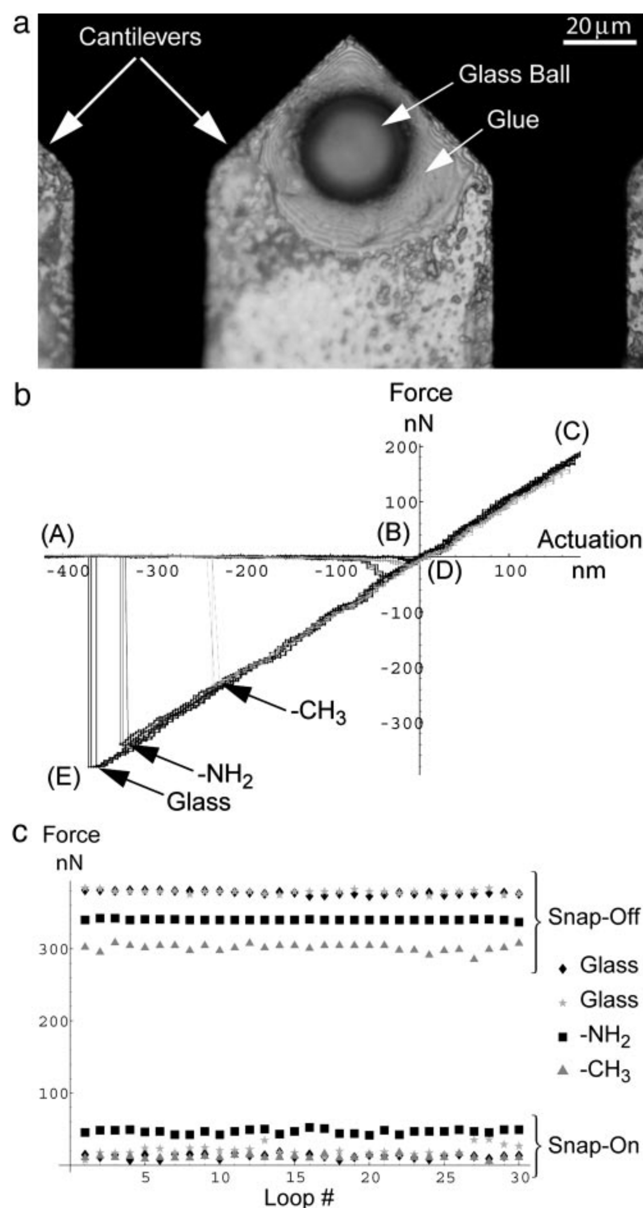

Fig. 4. Force-distance studies with the single-chip AFM. (*a*) Spherical glass beads (20 μm diameter) affixed to the cantilever end for force-distance measurements. The contact radius is $\approx$100 nm, and the contact area is 0.03 μm^2. (*b*) Four consecutive force response measurements of a glass surface and gold surfaces that were coated with a methyl-terminated and an amino-terminated undecanethiol SAM. The cantilever slowly approaches the surface (A) until the bead experiences an attractive force and comes in contact with the surface (snap-on, B). The load on the cantilever is increased to $\approx$160 nN (C), then the cantilever actuation is reversed. At (D) the force exerted on the sample changes from compressive to tensile, and at (E) the force is large enough to pull the bead off the surface (snap-off). (*c*) Snap-on and snap-off forces of 30 consecutive measurements (same cantilever). The mean values and standard deviations (in parentheses) of the snap-off forces amount to 379 nN (2.6 nN) for glass, 340 nN (0.9 nN) for the amino-terminated SAM, and 301 nN (4.9 nN) for the methyl-terminated SAM.

To achieve a well defined geometry of the cantilever surface to interact with the sample, spherical glass beads (20 μm diameter) were attached to the cantilever end (Fig. 4*a*). The radius of the contact spot is $\approx$100 nm, and the contact area has

been calculated to 0.03 μm^2 (25). Three identical glass beads were affixed to three cantilevers of the same chip for surface probing. The samples consisted of glass chips with gold patterns that were coated either with a methyl-terminated or an amino-terminated undecanethiol self-assembled monolayer (SAM). Fig. 4*b* shows the corresponding force response measurements. Four consecutive measurements for each sample surface are shown. Each data point represents the average of 12 recorded values. The data have been low-pass-filtered with a cutoff at 30-Hz corner frequency. It is evident from Fig. 4*c* that the glass bead (polar surface) interacts most intensely with the glass sample surface, to a lesser extent with the amino-terminated SAM, and most weakly with the nonpolar methyl-terminated SAM. The reproducibility of the measurements is shown in Fig. 4*d*. The "snap-on" and "snap-off" forces of 30 consecutive measurements (same cantilever) are displayed. The mean values and standard deviations (in parentheses) of the snap-off forces amount to 379 nN (2.6 nN) for glass, 340 nN (0.9 nN) for the amino-terminated SAM, and 301 nN (4.9 nN) for the methyl-terminated SAM. The same measurements conducted with the other two cantilevers of the same chip showed some fluctuations in the absolute values, but the relation between glass and amino-terminated SAM as well as that between glass and methyl-terminated SAM were preserved within 5–20% relative error.

For operating the monolithic AFM microsystem, only a simple circuit board is necessary to provide power supply stabilization and some reference voltages. There is no need for external signal processing capacity for either closed-loop imaging or open-loop force measurements. All operations can be performed on a chip. The digital interface connects the system to a computer for data capturing and visualization.

In summary, the AFM microsystem is a monolithic autonomous unit that allows for precise and fully controlled mechanical manipulation at nanometer/nanonewton resolution. The device is applicable to many fields including aerospace (low payload and low power), biotechnology (cell manipulation and force detection), and security (microbalance operation) applications. In particular, the force-distance mode can be used without a scanning stage so that surface and material characterization using, e.g., differently modified cantilevers is easy to perform. The chip can also be immersed in liquid phase. The device paves the way to developing other smart microsystems that will further bridge the gap to the nanoworld.

We thank Prof. Henry Baltes (on leave) for sharing laboratory resources and his ongoing stimulating interest in our work; former coworkers, notably Dirk Lange and Christoph Hagleitner, for developing a preversion of this fully integrated AFM chip; and Wendy Franks and Frauke Greve (Eidgenössische Technische Hochschule) for providing the SAM-modified surface and the neuron sample.

1. Binnig, G. & Rohrer, H. (1982) *Helv. Phys. Acta* **55,** 726–735.
2. Binnig, G., Quate, C. F. & Gerber, C. (1986) *Phys. Rev. Lett.* **56,** 930–933.
3. Meyer, E. & Heinzelmann, H. (1995) in *Scanning Tunneling Microscopy II*, eds. Wiesendanger, R. & Güntherodt, H. J. (Springer, Heidelberg), pp. 99–149.
4. Rief, M., Claussen-Schaumann, H. & Gaub, H. E. (1999) *Nat. Struct. Biol.* 6, 346–349.
5. Grandbois, M., Beyer, M., Rief, M., Claussen-Schaumann, H. & Gaub, H. E. (1999) *Science* **283,** 1727–1730.
6. Lehenkari, P. P., Charras, G. T., Nykänen, A. & Horton, M. A. (2000) *Ultramicroscopy* **82,** 289–295.
7. You, H. X., Lau, J. M., Zhang, S. & Yu, L. (2000) *Ultramicroscopy* **82,** 297–305.
8. Bowen, W. R., Hilal, N., Lovitt, R. W. & Wright, C. J. (1998) *Colloids Surf.* **136,** 231–234.
9. Minne, S. C., Manalis, S. R., Atalar, A. & Quate, C. F. (1996) *J. Vac. Sci. Technol.* **14,** 2456–2461.
10. Minne, S. C., Manalis, S. R. & Quate, C. F. (1999) *Bringing Scanning Probe Microscopy Up to Speed* (Kluwer, Boston).
11. Despont, M., Brugger, J., Drechsler, U., Durig, U., Haberle, W., Lutwyche, M., Rothuizen, H., Stutz, R., Widmer, R., Binnig, G., *et al*. (2000) *Sens. Actuators* **80,** 100–107.
12. Lutwyche, M., Andreoli, C., Binnig, G., Brugger, J., Drechsler, U., Haberle, W., Rohrer, H., Rothuizen, H., Vettiger, P., Yaralioglu, G. & Quate, C.F. (2000) *Sens. Actuators* **73,** 89–94.
13. Brugger, J. & de Rooij, N. F. (1992) *J. Microeng.* **2,** 218–224.
14. Linnemann, R., Gotszalk, T., Hadjiiski, L. & Rangelow, I. W. (1995) *Thin Solid Films* **264,** 159–164.
15. Gotszalk, T., Radojewski, J., Grabiec, P. B., Dumania, P., Shi, F., Hudek, P. & Rangelow, I. W. (1998) *J. Vac. Sci. Technol.* **16,** 3948–3953.
16. Jumpertz, R., Hart, A. V. D., Ohlsson, O., Saurenbach, F. & Schelten, J. (1998) *Microelectronic Eng.* **41**/**42,** 441–444.
17. Thaysen, J., Boisen, A., Hansen, O. & Bouwstra, S. (2000) *Sens. Actuators* **83,** 47–53.
18. Minne, S. C., Yaralioglu, G., Manalis, S. R., Adams, J. D., Zesch, J., Atalar, A. & Quate, C. F. (1998) *Appl. Phys. Lett.* **72,** 2340–2342.
19. Minne, S. C., Adams, J. D., Yaralioglu, G., Mannalis, S. R., Atalar, A. & Quate, C. F. (1998) *Appl. Phys. Lett.* **73,** 2340–2342.
20. Kim, Y. S., Nam, H. J., Cho, S. M., Hong, J. W., Kim, D. C. & Bu, J. U. (2003) *Sens. Actuators* **103,** 122–129.
21. Lange, D., Brand, O. & Baltes, H. (2002) *CMOS Cantilever Sensor Systems* (Springer, Berlin).
22. Akiyama, T., Staufer, U. & de Rooij, N. F. (2002) *Rev. Sci. Instrum.* **73,** 2643–2646.
23. Müller, T., Brandl, M., Brand, O. & Baltes, H. (2000) *Sens. Actuators* **84,** 126–133.
24. Volden, T., Zimmermann, M., Lange, D., Brand, O. & Baltes, H. (2004) *Sens. Actuators* **115,** 516–522.
25. Franks, W., Lange, D., Lee, S., Hierlemann, A., Spencer, N. & Baltes, H. (2002) *Ultramicroscopy* **91,** 21–27.